Measurement of $H \to b\bar{b}$ in Associated Production with the CMS Detector

by

Daniel Robert Abercrombie

B.S., Pennsylvania State University (2014)

Submitted to the Department of Physics
in partial fulfillment of the requirements for the degree of

Doctor of Philosophy

at the

MASSACHUSETTS INSTITUTE OF TECHNOLOGY

September 2020

Author .....
Department of Physics
June 10, 2020

Certified by .....
Christoph M. E. Paus
Professor of Physics
Thesis Supervisor

Accepted by .....
Nergis Mavalvala
Associate Department Head, Physics

Measurement of $H \to b\bar{b}$ in Associated Production with the CMS Detector

by

Daniel Robert Abercrombie

Submitted to the Department of Physics
on June 10, 2020, in partial fulfillment of the
requirements for the degree of
Doctor of Philosophy

Abstract

We measured $VH \to b\bar{b}$ with the CMS Detector.

Thesis Supervisor: Christoph M. E. Paus
Title: Professor of Physics

Acknowledgments

Thanks.

Contents

Chapter 1

Introduction

One of the most curious features of physics at small scales, which will likely frustrate students for the rest of time, is that certain sequences of events only have a probability of happening. There is no guarantee that an electron and a positron approaching each other at high energies will annihilate and produce an muon and an anti-muon. However, this event might still occur at a later time at with the exact same initial conditions. Furthermore, the observation of resonances where this is more likely to happen when the electron and positron approach each other at particular speeds does not mean that a Z boson was present in a given interaction. It just means that the weak component of the electroweak force significantly increases the probability of the muonic final state, given the total energy of the initial state. The sum of probabilities from different possible field interactions with particular initial conditions is the only thing we can measure. This is also only possible when observing many events with the same initial conditions.

This point is difficult to convey concisely, so many laypeople, as well as some practicing physicists, are confused by the terminology adopted by the field. But this distinction is relevant to the topic of this work. This document presents a measurement of a cross section. Cross section is the name given to the probability of an interaction occurring. Reported cross sections can be split up to describe different contributions to final states, and they can be collated into what are called "production cross sections" which describe the probabilities of particular intermediate states

"occurring" (even though intermediate states never exist in reality).

The main point is that if there exists some interesting particle, and it interacts with other particles, you can see an increased probability of certain initial states resulting in certain final states. This can teach the observer about the role of the interesting particle, without ever directly seeing it.

1.1 Measurement of the Higgs Cross Section

The purpose of the following document is to present the methods and results of measuring the strength of the coupling between the Higgs Boson and bottom quarks. In this context, the Higgs Boson makes up one of the previously mentioned intermediate states that cannot be shown as present in a given event. The cross section measurement relies on a number of physics processes that will be accounted for in this document.

To measure this coupling, the Higgs Boson must first be "produced" before measuring its coupling strength to bottom quarks. Since we are not technologically advanced enough to achieve this generation using bottom quarks directly, we use measured Higgs generation rates from normal constituents of protons. We constrain ourselves further by requiring that the Higgs is generated by associated production.

After the Higgs is generated, it can decay into a number of different particles. This work is only concerned with one kind of decay.

The math that this all relies on is presented in Chapter 2.

1.2 Motivation for the Measurement

This is Thomas Kuhn's "normal science".

Precision measurements are needed to be certain of what we think.

Precision measurements often lead to discrepancies that are explained by a fundamental shift in the model.

The Standard Model is a good one. It will not be fully replaced, but at worst

expanded upon. Just like Newton's Laws are still a reasonable approximation for General Relativity, The Standard Model is a good approximation for most things we have been able to interact with so far.

The only lingering questions are Dark Matter and Dark Energy, but there is no reason to assume that precise measurements of known phenomena will not lead to an explanation.

1.3 Historic Context

First, we have The Standard Model.

Parts were proven correct by the observation of the weak bosons.

The Higgs was observed in 2013.

The Higgs decaying to $b\bar{b}$was observed in 2018. [2]

1.4 Using the CMS Detector

The CMS detector is a general purpose detector used to make many observations of conditions unattainable on Earth outside of the LHC.

It has many stationary parts, and a couple of moving ones too.

This device is described in detail in Chapter 3.

Chapter 2

Theory

Before diving into the description of the experimental apparatus, an explanation of why it is expected to work is needed. There are many textbooks that cover the Standard Model, as there are many students who study it. Much of what follows is taken from the book by Mark Thompson [11].

The Standard Model Lagrangian can be defined as a sum of Lagrangians that each describe the interactions between different fermions and bosons. Equations of motion can be extracted from a Lagrangian $\mathcal{L}$ for a particle field ϕ_i using the Euler-Lagrange equations.

$$\delta_\mu \left(\frac{\delta \mathcal{L}}{\delta(\delta_\mu \phi_i)} \right) - \frac{\delta \mathcal{L}}{\delta \phi_i} = 0 \tag{2.1}$$

In the measurement of $H \to b\bar{b}$ in associated production, many components of the Standard Model are of interest. These will be introduced as needed. First, I will give a brief explanation of Higgs field's non-zero vacuum energy, a trait that makes the Higgs one of the central keystones to Standard Model. After that, the electroweak Lagrangian will be described since the cross section of associated production depends on the coupling of the Higgs Boson to the W and Z vector bosons. The coupling of the electroweak force to fermions is also important to understand both the generation of these intermediate states and the resulting final state that the CMS detector records.

Another important factor for this work is a the decay of the Higgs boson itself into bottom quarks. This depends on the Higgs directly coupling to fermions. Finally, we will briefly consider the part of the Lagrangian describing the strong force. Since the LHC is a hadron collider, understanding of the strong force is required to extract data from LHC collisions.

2.1 The Higgs Mechanism

In both of these components of the Standard Model Lagrangian, the Higgs coupling actually gives the vector bosons and massive fermions their mass [4, 7, 8]. (In this work, neutrinos can be treated as massless.) The granting of mass happens for two reasons: the Higgs field has a non-zero vacuum expectation value, and the Higgs field couples to vector boson and massive fermion fields.

The Higgs can be described as two complex scalar fields in a weak isospin doublet with a quartic potential. The Lagrangian for a free Higgs is then

$$\mathcal{L} = (\delta_\mu \phi)^\dagger (\delta^\mu \phi) - (\mu^2(\phi^\dagger \phi) + \lambda(\phi^\dagger \phi)^2) \tag{2.2}$$

Through the virial theorem, the potential has a minimum value when

$$\phi^\dagger \phi = \frac{-\mu^2}{2\lambda} = \frac{v^2}{2} \tag{2.3}$$

This potential of the Higgs field breaks the SU(2) $\times$ U(1) symmetry of the Standard Model Lagrangian. Through this non-zero vacuum expectation value, the Higgs then has a constant influence in other parts of the Standard Model Lagrangian. For this measurement, three interactions that the Higgs makes with this influence need to be considered: the Higgs interacting with itself, the Higgs interacting with the electroweak vector bosons, and the Higgs interacting with quarks.

The first two interactions manifest in the Lagrangian when we force the SU(2) $\times$ U(1) symmetry on the Lagrangian in Equation (2.2). The derivatives must be

replaced.

$$\delta_\mu \to D_\mu = \delta_\mu + i\frac{g_W}{2}\boldsymbol{\sigma}\cdot\mathbf{W}_\mu + ig'\frac{Y}{2}B_\mu \tag{2.4}$$

ϕ can be rewritten to satisfy the vacuum expectation value in the gauge that will give us the massless neutral boson known as a photon.

$$\phi(x) = \frac{1}{\sqrt{2}}\begin{pmatrix} 0 \\ v + h(x) \end{pmatrix} \tag{2.5}$$

This leads to the following expansion for the kinetic term of the Lagrangian.

$$\begin{aligned}(D_\mu\phi)^\dagger(D^\mu\phi) =& \frac{1}{2}(\delta_\mu h)(\delta^\mu h) + \frac{1}{8}g_W^2(W_\mu^{(1)} + iW_\mu^{(2)})(W^{(1)\mu} - iW^{(2)\mu})(v+h)^2 \\ &+ \frac{1}{8}(g_W W_\mu^{(3)} - g'B_\mu)(g_W W^{((3)\mu} - g'B^\mu)(v+h)^2\end{aligned} \tag{2.6}$$

Terms that are quadratic in terms of the gauge boson fields reveal the mass of the fields. Taking $h(x) \to 0$, the terms for $W^{(1)}$ and $W^{(2)}$ are the just

$$\frac{1}{4}g_W^2 v^2 W_\mu^{(1)}W^{(1)\mu} \quad \text{and} \quad \frac{1}{4}g_W^2 v^2 W_\mu^{(2)}W^{(2)\mu},$$

giving the mass.

$$m_W = \frac{1}{2}g_W v \tag{2.7}$$

The quadratic terms for $W^{(3)}$ and B mix to give a non-diagonal mass matrix $\mathbf{M}$.

$$\frac{v^2}{8}\begin{pmatrix} W_\mu^{(3)} & B_\mu \end{pmatrix}\mathbf{M}\begin{pmatrix} W^{(3)\mu} \\ B^\mu \end{pmatrix} = \frac{v^2}{8}\begin{pmatrix} W_\mu^{(3)} & B_\mu \end{pmatrix}\begin{pmatrix} g_W^2 & -g_W g' \\ -g_W g' & g'^2 \end{pmatrix}\begin{pmatrix} W^{(3)\mu} \\ B^\mu \end{pmatrix} \tag{2.8}$$

The non-diagonal matrix allow $W^{(3)}$ and B to mix. Physical states must be represented by a diagonal Hamiltonian. Diagonalizing the term above gives masses of the

physical states.

$$\frac{1}{8}v^2\begin{pmatrix}A_\mu & Z_\mu\end{pmatrix}\begin{pmatrix}0 & 0\\ 0 & g_W^2+g'^2\end{pmatrix}\begin{pmatrix}A^\mu\\ Z^\mu\end{pmatrix}=\frac{1}{2}\begin{pmatrix}A_\mu & Z_\mu\end{pmatrix}\begin{pmatrix}m_A^2 & 0\\ 0 & m_Z^2\end{pmatrix}\begin{pmatrix}A^\mu\\ Z^\mu\end{pmatrix} \tag{2.9}$$

This gives us the masses of the neutral gauge bosons.

$$m_A=0 \quad \text{and} \quad m_Z=\frac{1}{2}v\sqrt{g_W^2+g'^2} \tag{2.10}$$

From the simple act of requiring SU(2) $\times$ U(1) symmetry on the Lagrangian of a scalar doublet with non-zero vacuum expectation value, the masses of all the electroweak gauge bosons have been produced.

2.2 Associated Production

The next thing to consider is the couplings also produced by this process. The couplings will allow us to determine more precisely the parameters above by measuring cross sections.

The physical states of W^+ and W^- bosons can be written as the raising and lowering operators for isospin.

$$W^\pm=\frac{1}{\sqrt{2}}\left(W^{(1)}\mp iW^{(2)}\right) \tag{2.11}$$

The second term of Equation (2.6) can be further expanded.

$$\frac{1}{4}g_W^2W_\mu^-W^{+\mu}(v+h)^2=\frac{1}{4}g_W^2v^2W_\mu^-W^{+\mu}+\frac{1}{2}g_W^2vW_\mu^-W^{+\mu}h+\frac{1}{4}g_W^2W_\mu^-W^{+\mu}h^2 \tag{2.12}$$

The second term on the right hand side of Equation (2.12) gives us the coupling strength of a vertex with a Higgs and two W bosons.

$$g_{HWW}=\frac{1}{2}g_W^2v=g_Wm_W \tag{2.13}$$

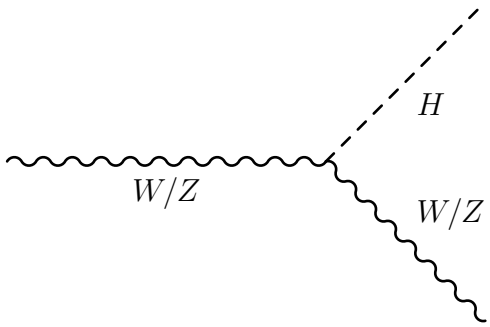

Figure 2-1: Above is the Feynman diagram for associated production. The W or Z boson radiates a Higgs boson. Both bosons later decay into particles detected by CMS.

The coupling to the Z boson can also be found from Equation (2.9) by substituting $(v+h)^2$ back in for v^2 and extracting the terms proportional to $hZ_\mu Z^\mu$.

$$g_{HZZ} = \frac{1}{2}\left(g_W^2 + g'^2\right) v = \sqrt{g_W^2 + g'^2} m_Z \tag{2.14}$$

When arranged in a way that the W or Z boson radiates the Higgs, as opposed to a Higgs decaying into a pair of W or Z bosons, the process is called associated production or *Higgstrahlung*. The vertex showing associated production is pictured in Figure 2-1.

2.2.1 Production Mechanisms of Vector Bosons

The W and Z bosons are themselves intermediate states, never existing in a directly observable manner. They must be produced through interacts with stable fermions. Since the LHC is a hadron collider, considering the vector bosons' couplings with quarks would be most relevant.

Quarks are fermions that couple to each other through the strong force, resulting from a SU(3) symmetry. There are three generations of quarks each consisting of a pair of quark types. Their mass eigenstates are denoted as down-type or up-type. Table 2.1 displays some of the characteristics of these quarks. A feature of quarks is that their mass eigenstates do not match their weak eigenstates. There is a mixing among the down-type quarks that is parametrized by the Cabibbo-Kobayashi-

Table 2.1: The quarks and some stuff about them.

	1st gen.	2nd gen.	3rd gen.	Q	$I_W^{(3)}$
down-type	d	s	b	$-\frac{1}{3}$	$-\frac{1}{2}$
up-type	u	c	t	$+\frac{2}{3}$	$+\frac{1}{2}$

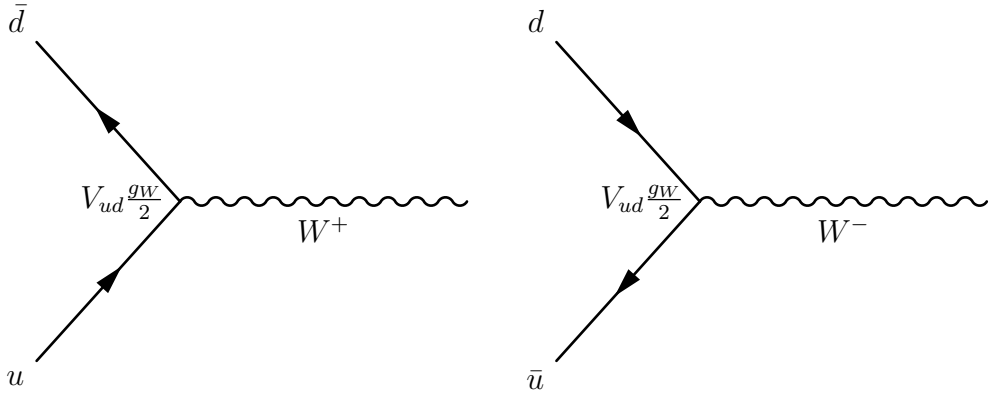

Figure 2-2: Above are diagrams for generating W^+ and W^- bosons. the u and d quarks in the diagram can be replaced with any up-type or down-type quark, respectively. The CKM matrix element would in the vertex element would be changed accordingly.

Maskawa (CKM) matrix.

$$\begin{pmatrix} d' \\ s' \\ b' \end{pmatrix} = \begin{pmatrix} V_{ud} & V_{us} & V_{ub} \\ V_{cd} & V_{cs} & V_{cb} \\ V_{td} & V_{ts} & V_{tb} \end{pmatrix} \begin{pmatrix} d \\ s \\ b \end{pmatrix} \tag{2.15}$$

The mass eigenstates are denoted as d, s, and b, while d', s', and b' are the weak eigenstates. This mixing allows quarks to change generations through interaction with $W^{\pm}$ bosons, which raise or lower the weak isospin. The following is the charge current vertex interaction.

$$-i\frac{g_W}{\sqrt{2}} \begin{pmatrix} \bar{u} & \bar{c} & \bar{t} \end{pmatrix} \gamma^\mu \frac{1}{2}(1-\gamma^5) \begin{pmatrix} V_{ud} & V_{us} & V_{ub} \\ V_{cd} & V_{cs} & V_{cb} \\ V_{td} & V_{ts} & V_{tb} \end{pmatrix} \begin{pmatrix} d \\ s \\ b \end{pmatrix}$$

The vertices for this interaction is shown in Figure 2-2 arranged in a way to show the processes of generating a W^+ or W^- boson from annihilating quarks. The γ

matrices in the interaction are present because the SU(2) component of the Standard Model only interacts with left-handed fermions and right-handed anti-fermions. For this reason, the SU(2) component is more accurately labelled $\mathrm{SU}(2)_L$. From Equation (2.11), the $W^{\pm}$ bosons are completely made up of the $W^{(1)}$ and $W^{(2)}$ components of the $\mathrm{SU}(2)_L$, so they also only interact with left-handed fermions and right-handed anti-fermions.

Both the photon and the Z boson mix the $\mathrm{SU}(2)_L$ and U(1) components of the Standard Model. Production of the Z needs to be directly understood for this measurement, but it is more straightforward to determine the strength of the Z couplings to left- and right-handed fermions by exploiting the symmetry of photon interactions. That is, the photon interacts the same with left and right handed charged fermions, and not at all with neutral fermions. This is shown directly with experiments with leptons. The charged leptons, electrons, muons, and taus, interact with photons, while the respective neutrinos do not. From the mixing in Equation (2.8), the photon and Z fields can be expressed as the following.

$$A_\mu = B_\mu \cos\theta_W + W^{(3)}_\mu \sin\theta_W \tag{2.16}$$

$$Z_\mu = -B_\mu \sin\theta_W + W^{(3)}_\mu \cos\theta_W \tag{2.17}$$

θ_W is known as the weak mixing angle. The relative strengths of the B and $W^{(3)}$ couplings are determined directly through lepton electro-magnetic characteristics, keeping in mind that $W^{(3)}$ only interacts with left handed particles. The following are the electro-magnetic interaction strengths of left- and right-handed electrons and neutrinos.

$$e_L: \qquad Qe = \frac{1}{2} g' Y_{e_L} \cos\theta_W - \frac{1}{2} g_W \sin\theta_W \tag{2.18}$$

$$\nu_L: \qquad 0 = \frac{1}{2} g' Y_{\nu_L} \cos\theta_W - \frac{1}{2} g_W \sin\theta_W \tag{2.19}$$

$$e_R: \qquad Qe = \frac{1}{2} g' Y_{e_R} \cos\theta_W \tag{2.20}$$

$$\nu_R: \qquad 0 = \frac{1}{2} g' Y_{\nu_R} \cos\theta_W \tag{2.21}$$

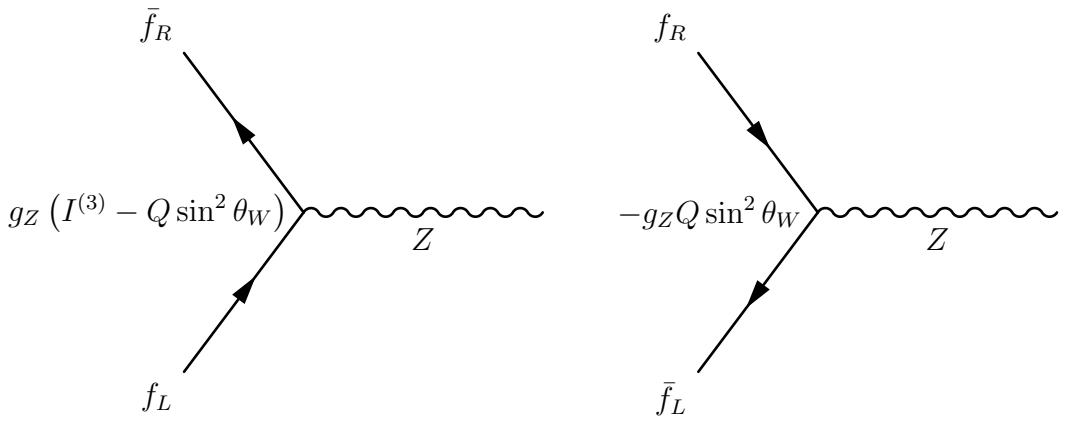

Figure 2-3: Above are diagrams for generating Z bosons. Left- and right-handed fermions are both coupled to, but with different coupling strengths.

Y_{e_L} and Y_{ν_L} must be equal to maintain $\mathrm{SU}(2)_L$ symmetry. To satisfy these contraints, the follow definition of Y is needed.

$$Y = 2\left(Q - I_W^{(3)}\right) \tag{2.22}$$

The following relationship also arises from these experimental constraints.

$$e = g_W \sin\theta_W = g' \cos\theta_W \tag{2.23}$$

Returning to the Z boson, from Equation (2.17), and defining

$$g_Z = \frac{e}{\sin\theta_W \cos\theta_W}, \tag{2.24}$$

we have the following couplings to left- and right-handed fermions.

$$-\frac{1}{2}g' \sin\theta_W (Y_{f_L}\bar{u}_L\gamma^\mu u_L + Y_{f_R}\bar{u}_R\gamma^\mu u_R) + I_W^{(3)} g_W \cos\theta_W \left(\bar{u}_L\gamma^\mu u_L\right) = g_Z\left(\left(I^{(3)} - Q\sin^2\theta_W\right)\bar{u}_L\gamma^\mu u_L - Q\sin^2\theta_W \bar{u}_R\gamma^\mu u_R\right) \tag{2.25}$$

Now the coupling of the Z to left- and right-handed quarks can be calculated from Table 2.1, remembering that $I_W^{(3)}$ for right-handed fermions is 0. Diagrams showing the interaction strengths of fermion-Z vertices are shown in Figure 2-3.

Thus vector bosons couple to quarks, the constituents of hadrons, which means

they can be produced at the LHC. As mentioned earlier in this section, quarks interact through an SU(3) symmetry that results in the strong force. The three states that this symmetry supports are known as color states, and they are labelled red, green, and blue, or r, g, and b. The resulting gauge bosons are known as gluons, and they carry the following color states.

$$r\bar{g}, g\bar{r}, r\bar{b}, b\bar{r}, g\bar{b}, b\bar{g}, \frac{1}{\sqrt{2}}(r\bar{r} - g\bar{g}) \text{and} \frac{1}{\sqrt{6}}(r\bar{r} + g\bar{g} - 2b\bar{b})$$

At low energy, the coupling constant for the strong force is on the order of unity. This leads to color confinement, so that quarks an appreciable distance apart do not interact with each other. To achieve this, all observable hadronic states are color singlets. The most common hadronic states are mesons, made of a quark/anti-quark pair with the color singlet state

$$\psi(q\bar{q}) = \frac{1}{\sqrt{3}}(r\bar{r} + g\bar{g} + b\bar{b}), \tag{2.26}$$

and baryons, made of three quarks with the following color singlet state.

$$\psi(qqq) = \frac{1}{\sqrt{6}}(rgb - rbg + gbrgrb + brg - bgr) \tag{2.27}$$

Baryons can also be composed of three anti-quarks, which has a state corresponding to Equation (2.27), but with anti-color.

For this measurement, protons are collided at the LHC. The proton consists of two u quarks, and one d quark. Since the three quarks inside the proton interact strongly, there are also many virtual gluons and quark/anti-quark pairs present at all times. The quantity and energies of all these partons are not able to be calculated since QCD is non-perturbative. They can be measured in deep inelastic scattering experiements though. In these, electrons are scattered off of protons, and parton distribution functions (PDFs) can be measured. The PDFs for protons are shown in Figure 2-4.

From these things, we can predict the cross section of generating W and Z bosons

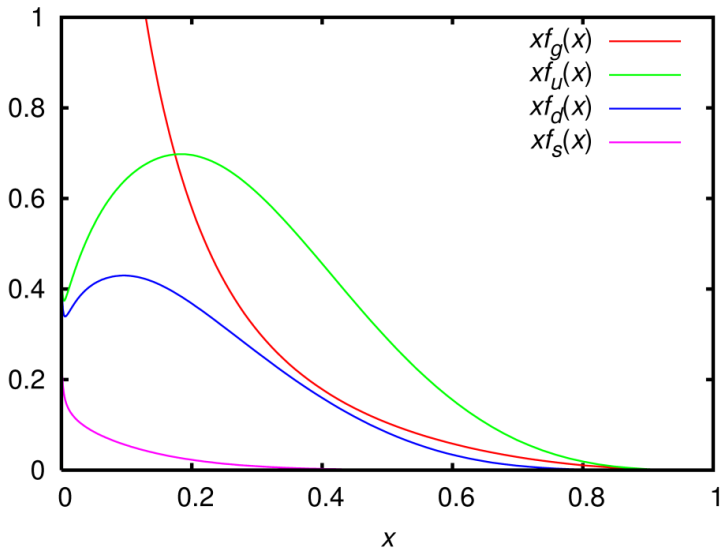

Figure 2-4: The P.D.F.

at the LHC. These need to be very massive though, since they're going to radiate a Higgs. This complicates the calculation a bit.

2.2.2 Decay Channels of Vector Bosons

Due to the couplings described in Section 2.2.1, the vector bosons decay into quarks. However, in the hadronic environment produced at the LHC these are not the best indicators of a vector boson intermediate state. This measurement uses leptonic decays in the final state since the contributions of the vector boson intermediate states to leptonic final states of appropriate kinematics are significantly larger.

2.3 Characteristics of the Higgs

What we are ultimately interested in measuring is the contribution of the Higgs intermediate state to the final state of $b\bar{b}$.

2.3.1 Energy Spectrum

2.3.2 Decay to $b\bar{b}$

2.4 Other Relevant Standard Model Processes

There are other processes that must be acknowledged in order to explain how the CMS detector works.

Chapter 3

The CMS Detector

The Compact Muon Solenoid (CMS) detector is a complex device located at the LHC. Ideally, a lot of time could be saved for the reader by only detailing the parts of the detector that are relevant for the analysis presented in this work. Unfortunately, a characteristic of contemporary collider measurements is that almost all sub-systems of the detector are used to make the final measurement.

A brief overview of all the detector subsystems are therefore presented in this chapter. A curious reader can learn more about the design and motivations for said design in the TDR [1].

3.1 Associated Production at the LHC

Before describing the devices that are used to observe and record events, the method of generating interesting events must be described. The CMS detector is located at the Large Hadron Collider (LHC). Described in detail in multiple publications [5], a brief description is given here.

The LHC, with a circumference of 26.7 km, is large enough to be considered located in multiple towns and countries, but it will suffice to say it is near Geneva, Switzerland at the European Organization for Nuclear Research (CERN), the main campus of which is addressed in Meyrin, Switzerland. This campus itself also spans the border between Switzerland and France.

Quark interactions can lead to Vector boson production, since the protons are at high energy.

Virtual vector bosons can radiate a Higgs.

This happens along with additional event stuff, caused by breaking apart the protons and pileup.

3.2 Observables of Associated Production

We can count charged leptons or infer neutrinos to tag vector bosons.

We are interested in Higgs to $b\bar{b}$.

3.3 Detector Requirements

We need to identify interesting particles, be able to reconstruct missing transverse momentum, and remove pileup.

3.3.1 Particle Types and Energies

3.3.2 Pileup Conditions at the LHC

3.4 Detector Design

3.4.1 Silicon Pixel Detector

3.4.2 ECAL

3.4.3 HCAL

3.4.4 Muon Chambers

3.5 Detector Performance

3.5.1 Test Beam Performance

3.5.2 Trigger

3.5.3 Online Calibration

3.6 Data Format

3.6.1 Event Reconstruction

3.6.2 Offline Calibration

3.7 Accessing Data

Chapter 4

Simulation

4.1 Backgrounds to the Analysis

In order to effectively measure Higgs production, we need to be able to accurately estimate other events that end up in our selection.

4.2 Event Generation

We use different generators.

Details in Appendix D.

4.2.1 Tree Level Simulation

4.2.2 Parton Showers

4.3 Detector Simulation

4.4 Corrections to Simulation

4.4.1 Smearing

Muons

Electrons

Jets

4.4.2 Selection Efficiencies

4.4.3 Control Regions

Light Flavor Jets

Heavy Flavor Jets

$t\bar{t}$

Chapter 5

Event Selection

5.1 Object Definitions

Section 3.6.1 describes how detector responses are linked to possible physical particles. We want to remove false positives, so here are some tighter requirements for counting for event selection.

Once we have our objects defined, we can count them.

5.1.1 Muons

Muons can show up in weakly decaying jets, so we're only interested in isolated ones here.

5.1.2 Electrons

Electrons do the same thing as muons, but messier because the ECAL isn't as clean as the muon chambers.

5.1.3 Jets

Jets are messier still.

Pileup removal is a big deal here.

5.1.4 MET

MET is corrected.

5.1.5 Undesirable Particles

There are certain particles that we do not want present. We make very loose selections for those and veto on them.

Photons

Tau Leptons

5.2 Removal of QCD

We have some cuts across the board on our objects in order to remove events that are just QCD.

5.3 Categories of Vector Boson Decay

Now that we are ready to count, we can count leptons in order to characterise potential vector bosons.

5.3.1 0 Leptons

5.3.2 1 Lepton

5.3.3 2 Leptons

5.4 Topology of Higgs Decay

5.4.1 Resolved Jets

We reconstruct two b jets.

5.4.2 Boosted Jet

When the Higgs has very high p_T, the jet clustering algorithms can find both daughter particles as being part of a single jet.

Chapter 6

Analysis Results

6.1 Systematic Uncertainties

6.2 Combination Fit Method

6.3 Results

Chapter 7

Conclusions

Appendix A

Detector Projects

Each collaborator must contribute to the operation of the CMS detector before his or her name is added to the author list. The operation of the detector is distinct from analyzing the data generated by the detector, so all collaborators must adopt some role outside of being a physicist.

This appendix details projects I completed in order to contribute to the operation of the CMS detector. The first project presented is the Dynamo Consistency project. It is a plugin for the dynamic data management system Dynamo [9] that compares the inventory of files Dynamo expects at a site with the files that are actually at a site. The other project described is known as Workflow Web Tools. This is a dynamic web server that displays errors reported by the CMS computing infrastructure to operators, and allows those operators to perform corrective actions through the web page. Workflow Web Tools also tracks operator actions for future use in training various machine learning models. Both projects produced software packages written in Python [12,13] and available through the Python Package Index (PyPI) as `dynamo-consistency` and `workflowwebtools`.

A.1 Dynamo Consistency

[3] [10]

A.2 Workflow Web Tools

Appendix B

Physics Calculations

Appendix C

Data Format

Appendix D

Generator Parameters

Appendix E

Data Card

Bibliography

[1] The CMS Collaboration. *CMS Physics: Technical Design Report Volume 1: Detector Performance and Software.* Technical Design Report CMS. CERN, Geneva, 2006.

[2] The CMS Collaboration. Observation of higgs boson decay to bottom quarks. *Physical Review Letters*, 121(12), Sep 2018.

[3] Alvise Dorigo, Peter Elmer, Fabrizio Furano, and Andrew Hanushevsky. Xrootd-a highly scalable architecture for data access. *WSEAS Transactions on Computers*, 1(4.3):348–353, 2005.

[4] F. Englert and R. Brout. Broken symmetry and the mass of gauge vector mesons. *Phys. Rev. Lett.*, 13:321–323, Aug 1964.

[5] Lyndon Evans and Philip Bryant. LHC machine. *Journal of Instrumentation*, 3(08):S08001–S08001, aug 2008.

[6] S. L. Glashow, J. Iliopoulos, and L. Maiani. Weak interactions with lepton-hadron symmetry. *Phys. Rev. D*, 2:1285–1292, Oct 1970.

[7] G. S. Guralnik, C. R. Hagen, and T. W. B. Kibble. Global conservation laws and massless particles. *Phys. Rev. Lett.*, 13:585–587, Nov 1964.

[8] Peter W. Higgs. Broken symmetries and the masses of gauge bosons. *Phys. Rev. Lett.*, 13:508–509, Oct 1964.

[9] Yutaro Iiyama, Benedikt Maier, Daniel Abercrombie, Maxim Goncharov, and Christoph Paus. Dynamo – handling scientific data across sites and storage media, 2020.

[10] Erwin Laure, A Edlund, F Pacini, P Buncic, M Barroso, A Di Meglio, F Prelz, A Frohner, O Mulmo, A Krenek, et al. Programming the grid with glite. Technical report, CERN, Geneva, Switzerland, 2006.

[11] Mark Thomson. *Modern particle physics.* Cambridge University Press, Cambridge, 2013.

[12] Guido Van Rossum and Fred L. Drake. *Python 3 Reference Manual.* CreateSpace, Scotts Valley, CA, 2009.

[13] Guido Van Rossum and Fred L Drake Jr. *Python reference manual*. Centrum voor Wiskunde en Informatica Amsterdam, 1995.